Poster contributions of the "Advanced Lectures on the Starburst-AGN Connection", Eds. R. Mújica, I. Aretxaga & D. Kunth, 2001, INAOE Electronic Edition (http://www.inaoep.mx/∼agn00/posters.html), pp. 47-50

Starburst Activity in Seyfert 2 Galaxies: UV–X-ray emission in NGC1068

E. Jiménez Bailón[1], **J.M. Mas Hesse**[1] **and M. Santos Lleó**[2]

[1] LAEFF-INTA, Estación de Seguimiento de Satélites de Villafranca del Castillo, Madrid, Spain
[2] XMM Science Operations Center, Astrophysics Division, ESA Space Science Department, P.O. Box 50727, E-28080 Madrid, Spain.

Abstract. In certain galaxies with Seyfert 2 nuclei, the UV continuum has been found to be essentially dominated by starburst episodes distributed around their central regions. Our goal is to compare the overall measured X-ray emission with the expected contribution associated to the starbursts, in order to disentangle the relative intensity of both the starburst and active nucleus high energy components. In this paper we present the method and discuss the preliminary results obtained on the prototypical Seyfert 2 galaxy NGC1068.

1. Introduction

According to the unified model of Seyfert galaxies, the observational differences between Seyfert 1 and 2 objects are mainly associated to the orientation of the line of sight with respect to the active nucleus and the surrounding dense torus (Antonucci et al. 1985, Tran 1995). According to this scenario, the UV continuum in Seyfert 2 galaxies would be completely blocked by the torus, so that we would detect only the radiation scattered from the hidden Seyfert 1 nucleus. Nevertheless, several studies in the last years (Mas-Hesse et al. 1995, Cid-Fernandes and Terlevich 1995, Colina et al. 1997, Heckman et al. 1995, González-Delgado et al. 1998) have shown that in several Seyfert 2 galaxies the main part of the UV continuum is produced by reddened circumnuclear young starbursts, located at typical distances of hundreds of parsecs from the nucleus (or less). In some of these objects it seems that only a very small fraction of the UV continuum emission could be attributed to the hidden Seyfert 1 nucleus. Therefore, there are observational evidences for the coexistence of both physical phenomena in the central region of Seyfert 2 galaxies: the hidden Seyfert 1 nucleus and the circumnuclear starbursts.

Considering the X ray emission of these objects, it would be contributed not only by the hidden nucleus, but also by the star-forming regions. The poor spatial resolution of most X-ray observations does not allow to separate the active nucleus emission from the contribution by circumnuclear starbursts. We have developed an indirect method to infer the X-ray emission associated to the starburst, in order to disentangle the contribution of the active galactic nucleus itself from the whole X ray emission.

In Sect. 2 we explain the method and the tools required. In order to test the feasibility of the technique we have applied it to NGC1068, the well-studied prototype of Seyfert 2 nuclei and in which circumnuclear starbursts have actually been identified (Neff et al. 1994, Thatte et al. 1997). In Sect. 3 we present the observational data and the results; we summarized in Sect. 4 our conclusions, after a short discussion of the results.

2. Description of the method

Our main goal is to quantify the relative contribution of the circumnuclear starbursts to the overall X-ray emission of the central region in Seyfert 2 nuclei. Assuming that the UV emission of the central region is dominated by a single starburst, we will use the evolutionary synthesis models developed by Cerviño et al. (2000) to compute an upper limit for the X-ray emission associated to the starburst. Comparing this prediction with the observed X-ray emission, it becomes possible to estimate the fraction of the emission originated in the central region associated to both the active nucleus and star forming processes themselves. The working method for the study of a Seyfert 2 nucleus consists of four steps:

- First, spatial and spectroscopical analysis of the UV emission in the central region of the Seyfert 2 galaxy. If UV imaging with enough spatial resolution is available, the circumnuclear starbursts will be located and measured, if any. Analysis of the UV continuum will yield a first estimate of the extinction and the strength of the starburst episodes.
- The X-ray luminosity of the nucleus is measured and characterized. Since usually the overall emission of the whole galaxy will be integrated, we should try to separate by spectral fitting the different components contributing to the total X-ray emission: a thermal component associated to the starbursts, and a non-thermal component due to the active nucleus, which might be partially absorbed by the dense torus.

– Comparison with the predictions of evolutionary synthesis models allows then to constrain the properties of the starbursts, and to extrapolate the expected emission in the soft and hard X-ray bands.
– Finally, comparison with the measured X-ray luminosity will provide an upper limit for the fraction of emission attributed to the starburst.

3. NGC1068: Observational data and results

As NGC1068 is one of the nearest Seyfert 2 galaxies and because the galactic extinction in its line of sight is very weak, numerous and very accurate observations at different wavelength ranges have been performed. Since the discovery of its hidden Seyfert 1 nucleus by polarized light studies (Antonucci & Miller 1985), NGC1068 became the strongest observational evidence for unified models and the prototype of Seyfert 2 nuclei. In addition, NGC1068 presents very active star forming episodes at typical distances of kpc (Neff et al. 1994), and more compact circumnuclear starbursts (Thatte et al. 1997). Therefore, NGC1068 is the most appropriate target for our study, since there are numerous observational data and the central region harbors intense starbursts. NGC1068 is placed at 14.4 Mpc, (z = 0.0038), and has a bolometric luminosity of $2 \times 10^{11} L_\odot$.

3.1. UV and X-ray observational data

NGC1068 was imaged in the UV by the *UIT* (Ultraviolet Imaging Telescope). This image of NGC1068 and the location of the detected starbursts can be seen in Figure 1. The identification of the different knots has been taken from Neff et al. (1994).

For the spectral analysis of the different regions we have combined calibrated data from the *IUE* (International Ultraviolet Explorer) and *HUT* (Hopkins Ultraviolet Telescope) archives. We selected the *IUE* spectra taken with its large slit (10″ × 20″; ∼ 700 × 1000 pc) and centered in the nucleus of NGC1068, a total of 11 spectra. Both short and long wavelength (1150 Å - 1980 Å; 1850 Å - 3350 Å) spectra have been analyzed. The weighted average spectrum is presented in Figure 2. This spectrum has been corrected from galactic extinction assuming $E(B-V) = 0.034$ (Schlegel et al. 1998). Taking into account the positions of the starbursts identified on the *UIT* image and the aperture of the *IUE* slit, it can be concluded that this spectrum includes the overall emission of the central region, with both the active nucleus and the compact starbursts, as well as part of the emission of the strong J knot.

One *HUT* observation with a circular aperture 30″ in diameter and a spectral range from 830 Å to 1850 Å has also been analyzed. In this case, the spectrum includes the emission originated in the innermost regions of NGC1068 and the most intense knot, J, as well as part of the emission coming from other intense knots: G, H and I. The *HUT* spectrum, corrected from galactic extinction, is shown in Figure 3.

Avoiding the emission and absorption lines, forth-order polynomials have been fitted to each spectrum. The fitted polynomials of the two spectra are plotted in Figures 2 and 3 and have been used as inputs for the synthesis models.

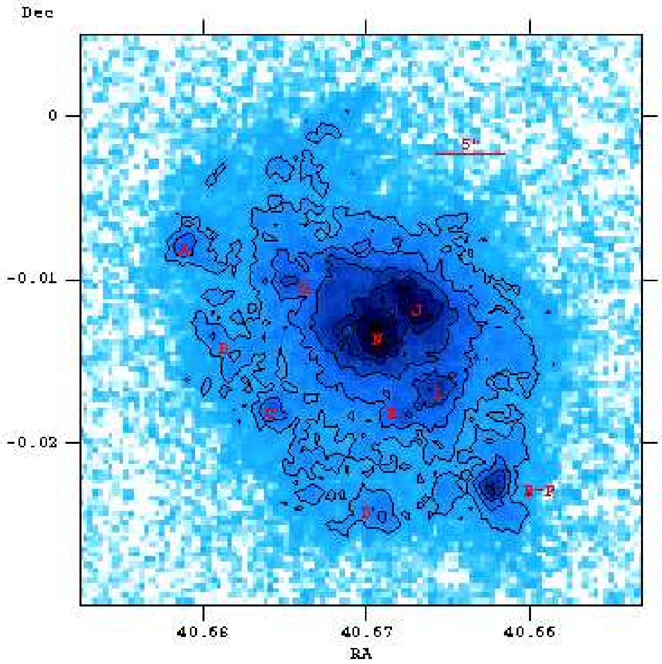

Fig. 1. Star forming knots in NGC1068. *UIT* image of NGC1068, taken with the B1 filter ($\lambda_{eff} = 1520$ Å, $\Delta\lambda = 354$ Å). North is up and east is left. 1 arcsec ≃ 70 pc.

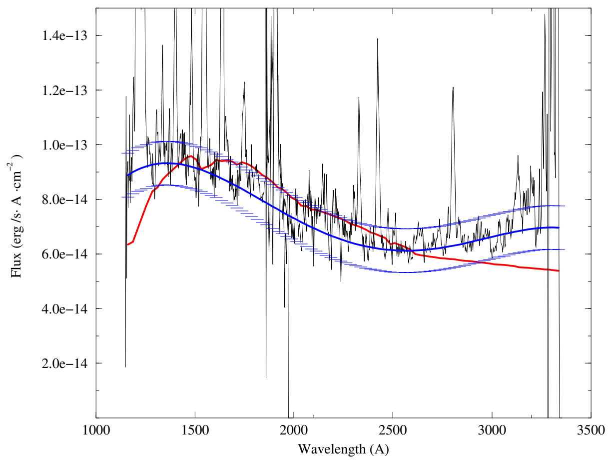

Fig. 2. ***IUE* spectrum of NGC1068.** The weighted average *IUE* spectrum is shown in black; in blue, the best fit continuum, with associated errors; and in red the continuum emission of the best fitting starburst.

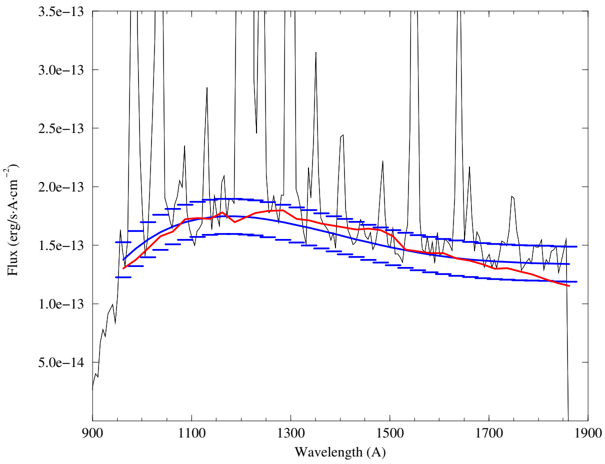

Fig. 3. ***HUT*** **spectrum of NGC1068.** The *HUT* spectrum is shown in black; in blue, the best fit continuum, with associated errors, and in red the continuum emission of the best fitting starburst.

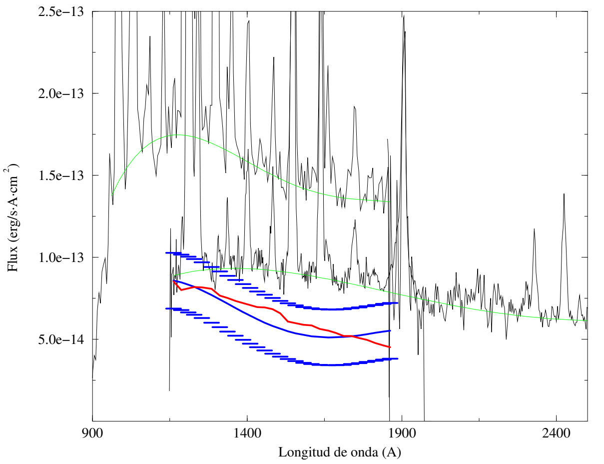

Fig. 4. Spectrum of NGC1068 for the region included between 700 - 1000 pc. The *IUE* and *HUT* spectra are shown in black, with their fit continuum in green; in blue, the difference of the previous continua, with associated error band, and in red the continuum emission of the best fitting starburst.

We have also computed the difference of the continuum in both apertures, just subtracting the fitted polynomials. This continuum represents the contribution of the star-forming knots in NGC1068 which are placed outside the *IUE* slit, but still within the central 1 kpc. This difference continuum and the fitted polynomial are represented in Figure 4.

We have considered an *ASCA* observation of NGC1068. The data have been fitted to a multicomponent model, including a power law, a Raymond-Smith plasma

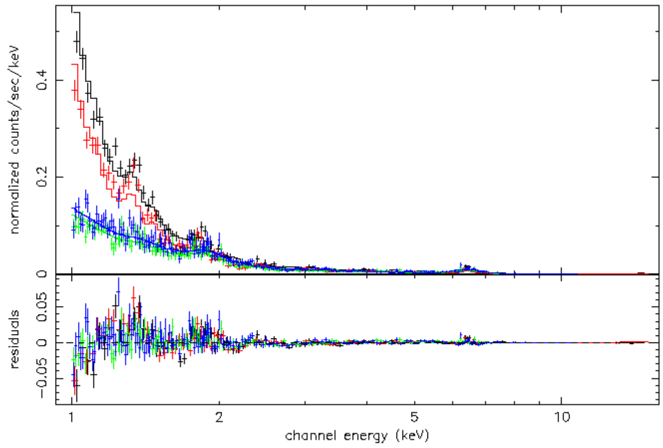

Fig. 5. ASCA X ray spectrum of NGC1068. The plot includes the observational data, the best fit model and the corresponding residuals for the four detectors.

Table 1. Best fitting model parameters. For the power law and the Raymond-Smith components, the normalization is given in $photons \cdot keV^{-1} \cdot cm^{-2}$ at 1 keV. The energy parameters units are keV, and the normalization for the Fe line is given in $photons \cdot cm^{-2}$ at 6.6 keV.

Power law	**Parameter**	**Error**
Index	1.994	0.05
Normalization	$1.1 \cdot 10^{-3}$	$0.1 \cdot 10^{-3}$
Raymond-Smith	**Parameter**	**Error**
kT	0.66	0.02
Normalization	$2.7 \cdot 10^{-3}$	$0.1 \cdot 10^{-3}$
Iron Line	**Parameter**	**Error**
Energy	6.56	0.02
ΔE	0.35	0.02
Normalization	$1.9 \cdot 10^{-4}$	$0.2 \cdot 10^{-4}$

and the iron emission line, as given Table 1. The original data, together with the best fit model and the corresponding residuals are shown in Figure 5. The *ASCA* data include the whole X-ray emission of the galaxy. The unabsorbed luminosities obtained for the two bands considered are given in Table 3.

3.2. Evolutionary synthesis models results

To compare the observational data with the predictions of evolutionary synthesis models we have considered the UV continuum measured on two areas: the central region, as integrated within the *HUT* slit, and the external region, obtained from the difference between the *HUT* and *IUE* continua. We have assumed that the UV continuum in both regions is dominated by single strong starbursts, and have tried to derive their properties by fitting the observed and the predicted UV continua. In this way we have obtained the starburst mass and age, and the extinction law and corresponding color excess of the star for-

Table 2. Fit values for the starbursts. For both assumed starbursts, an active region of SMC extinction law was found. The mass is given in $M_\odot$ units and the age in Myr. The fitting test performed was a χ^2 test, ν represents the degrees of freedom. The *HUT* region covers 1 kpc and the *HUT-IUE* from 700 - 1000 pc.

Region	E(B-V)	Age	Mass	χ^2	ν
HUT	0.09	2	$3.2 \cdot 10^6$	0.297	29
HUT-IUE	0.07	2	$1.0 \cdot 10^6$	0.0269	21

Table 3. Predicted X-ray luminosity. The soft and hard X ray luminosity predicted for the two regions of NGC1068 considered in this study. The observational data included for comparison correspond to the overall X-ray emission of the whole galaxy, as measured with *ASCA*.

Region	$L_{0.07-2.4\,keV}$ $erg \cdot s^{-1}$	$L_{2-10\,keV}$ $erg \cdot s^{-1}$
HUT	$\sim 1.5 \cdot 10^{41}$	$\sim 2 \cdot 10^{40}$
HUT-IUE	$\sim 4 \cdot 10^{40}$	$\sim 1 \cdot 10^{40}$
Observational luminosity	$1.1 \cdot 10^{42}$	$3 \cdot 10^{41}$

mation process that would better reproduce the observed UV properties. The parameters of the best fitting models are given in Table 2, together with the corresponding χ^2 values. The best-fitting continua are plotted on Figures 3 and 4. As it can be seen in Figure 2, it has not been possible to find a model that produce an acceptable good fit for the *IUE* spectrum. We list finally in Table 3 the expected X-ray emission as predicted by the evolutionary synthesis models, assuming that the UV continuum is dominated by the starburst contribution.

4. Discussion and conclusions

Comparison of the predicted and observational data on Table 3 leads to the following conclusions:

- Assuming that the whole UV emission originated in the central kpc of NGC1068 is due to a starburst of 2 Myr and $3.2 \cdot 10^6\, M_\odot$, this starburst could explain between 10% and 20% of the soft X-ray luminosity, but less than 7% of the hard X-ray emission.
- The star formation episodes located in the region between 700–1000 pc from the nucleus contribute to less than 4% to the total soft X-ray emission, assuming they can be modeled by a starburst around 2 Myr old having transformed around $10^6\, M_\odot$ in stars.
- Despite the evidence of stellar formation in the innermost region of NGC1068, (< 700 pc), its UV continuum could not be modeled by a starburst only, indicating that the contribution of the scattered component has to be significant. This result is in agreement with the conclusions of Crenshaw & Kraemer 2000, who using UV *STIS* observations show that the compact innermost region of NGC1068 seems to be dominated by reflected radiation from the hidden nucleus.
- The measured soft X-ray radiation in NGC1068 seems to be therefore dominated by emission reflected from the hidden active nucleus. Nevertheless, the star-forming episodes in its central region could be (at least partially) responsible for the thermal soft X-ray component identified on *ASCA* data by Bianchi et al. (2000). On the other hand, the hard X-ray emission of NGC1068 has to be fully originated by reflected emission, with a negligible contribution by starbursts.

An indirect method of measurement has been developed in order to disentangle the high energy contribution originated in the starbursts observed in the central region of numerous Seyfert 2 galaxies from the active nucleus emission itself. The proposed method has been probed with the prototype Seyfert 2 galaxy NGC1068, finding that the relative contribution of starbursts at UV–X-ray wavelengths is small, below 20%. We expect that in other Seyfert 2 galaxies, whose UV continuum is clearly dominated by massive stars, the relative contribution of starbursts to X-ray emission will be significantly higher, possibly becoming the dominant component.

References

Antonucci R. R. J., Miller J. S. 1985, ApJ 297, 621
Bianchi S., Matt G., Iwasawa K. 2000, MNRAS in press
Cerviño M., Mas-Hesse J. M., Kunth D. 2000, A&A in press
Cid-Fernandes R., Terlevich R. 1995 MNRAS 272, 423
Colina L., González Vargas M. L. , González Delgado R. M., Mas-Hesse J. M., Pérez E., Alberdi A. , Krabbe A., 1997, ApJ 488, L71
González-Delgado R. M., Heckman T., Leitherer C., Meurer G., Krolik J., Wilson A. S., Kinney A., Koratkar A. 1998, ApJ 505, 174
Heckman T., Krolik J., Meurer G., Calzetti D., Kinney A., Koratkar A., Leitherer C., Robert C, Wilson A. 1995, ApJ 452, 549
Crenshaw D. M., Kraemer S. B. 2000, ApJ 532, 247
Mas-Hesse J. M., Rodríguez-Pascual P. M., Sanz Fernández de Córdoba L., Mirabel I. F., Wamsteker W., Makino F., Otani C. 1995, A&A 298, 22
Neff S. G., Fanelli M., Roberts L. J., O'Connell R. W., Bohlin R., Roberts M. S., Smith A. M., Stecher T. P. 1994, ApJ 430, 545
Schlegel D. J., Finkbeiner D. P., Davis M. 1998, ApJ 500, 525
Thatte N., Quirrenbach A., Genzel R., Maiolino R., Tecza M. 1997, ApJ 490, 238
Tran H. 1995, ApJ 440, 565